Cylindrical 3D FDTD algorithm for the computation of low frequency transient eddy currents in MRI

A. Trakic[1], H. Wang[1], F. Liu[1], H. S. Lopez[1], S. Crozier[1]

[1]School of Information Technology and Electrical Engineering, The University of Queensland, Brisbane, QLD, Australia

Synopsis: In Magnetic Resonance Imaging (MRI), pulsing of magnetic field gradients induces time-varying eddy currents in nearby conductors. These secondary fields are a major cause of concern, since they degrade the image quality by causing misregistration and intensity/phase variations in both images and spectra. A numerical characterization of deleterious eddy current effects is vital for their compensation/control and further advancement of the MRI technology. A robust analysis scheme allows more complete design and optimisation of gradient coil/magnet combinations and provides indicative predictions of the pre-emphasis and B0-shift compensation waveforms required. We present a novel three-dimensional (3D) finite-difference time-domain (FDTD) method in cylindrical coordinates for modelling of low-frequency transient eddy currents and associated temporal side effects encountered in MRI.

Methods: The FDTD method is routinely used for high frequency applications, due to its simplicity and efficiency in wave models. In low frequency and high-resolution applications, however, Maxwell's formulations in standard FDTD form suffer from a prohibitively long execution time. Maxwell's equations are adapted to the low-frequency regime by downscaling the speed of light constant, which permits larger time steps while maintaining the validity of the Courant-Friedrich-Levy stability condition. The low-frequency FDTD scheme is formulated in cylindrical space, which avoids the presence of 'stair-case' errors typically associated with the FDTD computations in Cartesian coordinates [1]. Additionally, the scheme conforms well to the cylindrical structures used in MRI.

1. The central-differenced FDTD form of Maxwell's update equations in cylindrical coordinates can be written:

$$H_r\Big|_{i,j+\frac{1}{2},k+\frac{1}{2}}^{n+\frac{1}{2}} = H_r\Big|_{i,j+\frac{1}{2},k+\frac{1}{2}}^{n} + \frac{\Delta t}{\mu}\left(\frac{E_\varphi\Big|_{i,j+\frac{1}{2},k+1}^{n} - E_\varphi\Big|_{i,j+\frac{1}{2},k}^{n}}{\Delta z} - \frac{E_z\Big|_{i,j+1,k+\frac{1}{2}}^{n} - E_z\Big|_{i,j,k+\frac{1}{2}}^{n}}{r_i\Delta\varphi}\right)$$

$$E_r\Big|_{i+\frac{1}{2},j,k}^{n+1} = e^{-\sigma\Delta t/\varepsilon}E_r\Big|_{i+\frac{1}{2},j,k}^{n} + \frac{\Delta t}{\varepsilon}J_r\Big|_{i+\frac{1}{2},j,k}^{n+\frac{1}{2}} + \left(\frac{1-e^{-\sigma\Delta t/\varepsilon}}{\sigma}\right)\left(\frac{H_z\Big|_{i+\frac{1}{2},j+\frac{1}{2},k}^{n+\frac{1}{2}} - H_z\Big|_{i+\frac{1}{2},j-\frac{1}{2},k}^{n+\frac{1}{2}}}{r_{i+\frac{1}{2}}\Delta\varphi} - \frac{H_\varphi\Big|_{i+\frac{1}{2},j,k+\frac{1}{2}}^{n+\frac{1}{2}} - H_\varphi\Big|_{i+\frac{1}{2},j,k-\frac{1}{2}}^{n+\frac{1}{2}}}{\Delta z}\right)$$

$$H_\varphi\Big|_{i+\frac{1}{2},j,k+\frac{1}{2}}^{n+\frac{1}{2}} = H_\varphi\Big|_{i+\frac{1}{2},j,k+\frac{1}{2}}^{n} + \frac{\Delta t}{\mu}\left(\frac{E_z\Big|_{i+1,j,k+\frac{1}{2}}^{n} - E_z\Big|_{i,j,k+\frac{1}{2}}^{n}}{\Delta r} - \frac{E_r\Big|_{i+\frac{1}{2},j,k+1}^{n} - E_r\Big|_{i+\frac{1}{2},j,k}^{n}}{\Delta z}\right)$$

$$E_\varphi\Big|_{i,j+\frac{1}{2},k}^{n+1} = e^{-\sigma\Delta t/\varepsilon}E_\varphi\Big|_{i,j+\frac{1}{2},k}^{n} + \frac{\Delta t}{\varepsilon}J_\varphi\Big|_{i,j+\frac{1}{2},k}^{n+\frac{1}{2}} + \left(\frac{1-e^{-\sigma\Delta t/\varepsilon}}{\sigma}\right)\left(\frac{H_r\Big|_{i,j+\frac{1}{2},k+\frac{1}{2}}^{n+\frac{1}{2}} - H_r\Big|_{i,j+\frac{1}{2},k-\frac{1}{2}}^{n+\frac{1}{2}}}{\Delta z} - \frac{H_z\Big|_{i+\frac{1}{2},j+\frac{1}{2},k}^{n+\frac{1}{2}} - H_z\Big|_{i-\frac{1}{2},j+\frac{1}{2},k}^{n+\frac{1}{2}}}{\Delta r}\right)$$

$$H_r\Big|_{i,j+\frac{1}{2},k+\frac{1}{2}}^{n+\frac{1}{2}} = H_r\Big|_{i,j+\frac{1}{2},k+\frac{1}{2}}^{n} + \frac{\Delta t}{\mu}\left(\frac{E_\varphi\Big|_{i,j+\frac{1}{2},k+1}^{n} - E_\varphi\Big|_{i,j+\frac{1}{2},k}^{n}}{\Delta z} - \frac{E_z\Big|_{i,j+1,k+\frac{1}{2}}^{n} - E_z\Big|_{i,j,k+\frac{1}{2}}^{n}}{r_i\Delta\varphi}\right)$$

$$E_z\Big|_{i,j,k+\frac{1}{2}}^{n+1} = e^{-\sigma\Delta t/\varepsilon}E_z\Big|_{i,j,k+\frac{1}{2}}^{n} + \frac{\Delta t}{\varepsilon}J_z\Big|_{i,j,k+\frac{1}{2}}^{n+\frac{1}{2}} + \left(\frac{1-e^{-\sigma\Delta t/\varepsilon}}{r_i\sigma}\right)\left(\frac{r_{i+\frac{1}{2}}H_\varphi\Big|_{i+\frac{1}{2},j,k+\frac{1}{2}}^{n+\frac{1}{2}} - r_{i-\frac{1}{2}}H_\varphi\Big|_{i-\frac{1}{2},j,k+\frac{1}{2}}^{n+\frac{1}{2}}}{\Delta r} - \frac{H_r\Big|_{i,j+\frac{1}{2},k+\frac{1}{2}}^{n+\frac{1}{2}} - H_r\Big|_{i,j-\frac{1}{2},k+\frac{1}{2}}^{n+\frac{1}{2}}}{\Delta\varphi}\right)$$

Where Δr, $\Delta\phi$ and Δz are radial, azimuthal and axial cell dimensions, respectively. A general arrangement of EM field components in a cylindrical cell is illustrated in Figure 1. An alternate time-stepping expression involving exponential coefficients is used to replace the standard linear coefficients. This precludes any diffusion instabilities that may be caused by the exponential decay of propagating waves inside good conductors. The standard linear coefficients [2]:

$\frac{2\varepsilon - \sigma\Delta t}{2\varepsilon + \sigma\Delta t}$ and $\frac{2\Delta t}{2\varepsilon + \sigma\Delta t}$ are replaced with the following exponential coefficients, respectively: $e^{-\sigma\Delta t/\varepsilon}$ and $\frac{1-e^{-\sigma\Delta t/\varepsilon}}{\sigma}$, where $\varepsilon = \varepsilon_r(\alpha\varepsilon_0)$ and α is a scaling factor.

2. The adaptation of the conventional FDTD scheme to low frequency applications can be achieved by scaling up the permittivity and leaving the permeability of free space unchanged [3]. The downscaled speed of light constant c_α and stable time step Δt are then given by:

$$c_\alpha = \frac{1}{\sqrt{\alpha\mu_0\varepsilon_0}} \qquad \Delta t < \frac{k_t\sqrt{\alpha}}{c_\alpha\sqrt{\left(\frac{1}{\Delta r}\right)^2 + \left(\frac{1}{r_{\min}\Delta\varphi}\right)^2 + \left(\frac{1}{\Delta z}\right)^2}}$$

where α is a dimensionless scaling factor, μ_0 is the permeability of free space, ε_0 is the permittivity of free space, ε_α is the scaled free space permittivity, k_t is the safety coefficient (< 1) and $r_{\min}$ is the minimal radial component to be studied (here: $r_{\min} = 0.5\Delta r$).

3. The numerical singularity associated with the polar axis in cylindrical coordinates is removed by the use of series expansion for the field quantities in radial dimension [4]. The singular radial magnetic and azimuthal electric field components are approximated by the following regularity conditions:

$$H_r\Big|_{0,j+\frac{1}{2},k+\frac{1}{2}}^{n+\frac{1}{2}} = \frac{1}{N_\phi}\left(\sin\phi_{j+\frac{1}{2}}\sum_{m=0}^{N\phi}\left(H_\phi\Big|_{\frac{1}{2},m,k+\frac{1}{2}}^{n+\frac{1}{2}}\cos\phi_{m+\frac{1}{2}}\right) + \cos\phi_{j+\frac{1}{2}}\sum_{m=0}^{N\phi}\left(H_\phi\Big|_{\frac{1}{2},m,k+\frac{1}{2}}^{n+\frac{1}{2}}\sin\phi_{m+\frac{1}{2}}\right)\right)$$

$$E_\phi\Big|_{0,j+\frac{1}{2},k}^{n+1} = \frac{1}{N_\phi}\left(\cos\phi_{j+\frac{1}{2}}\sum_{m=0}^{N\phi}\left(E_r\Big|_{\frac{1}{2},m,k}^{n+1}\sin\phi_{m+\frac{1}{2}}\right) - \sin\phi_{j+\frac{1}{2}}\sum_{m=0}^{N\phi}\left(E_r\Big|_{\frac{1}{2},m,k}^{n+1}\cos\phi_{m+\frac{1}{2}}\right)\right)$$

The axial electric field component is obtained by considering Amperes law through a closed circular integral path of radius $0.5\Delta r$ around the polar axis:

$$E_z\Big|_{0,j,k+\frac{1}{2}}^{n+1} = \frac{2\varepsilon - \sigma\Delta t}{2\varepsilon + \sigma\Delta t}E_z\Big|_{0,j,k+\frac{1}{2}}^{n} + \left(\frac{4}{\Delta r N_\phi}\right)\left(\frac{2\Delta t}{2\varepsilon + \sigma\Delta t}\right)\sum_{m=0}^{N_\phi}H_\phi\Big|_{\frac{1}{2},m,k+\frac{1}{2}}^{n+\frac{1}{2}}$$

4. A split version PML absorbing boundary condition (PML-ABC) of cylindrical type has been adopted from Berenger's original PML theory based on Cartesian space [2]. In 3D cylindrical coordinates, only field components in radial and axial dimensions need to be considered in the PML region, which simplifies the 3D PML problem to only two dimensions. In order to retain the perfectly matched boundary condition at the air-PML interface, one should additionally scale the electric conductivity σ of the PML region by the same factor. The magnetic conductivity σ^* boundary condition is then given by:

$$\sigma^* = \frac{(\alpha\sigma)\mu_0}{\varepsilon_\alpha}$$

Results: The numerical scheme is verified against a FEMLAB benchmark involving a current carrying coil (radius = 0.03m, cross section = 0.002 x 0.005m) centred inside a hollow cylindrical metal shell (radius = 0.06m, thickness = 0.01m) with a material conductivity of 5e5 S/m. A 500Hz-trapezoidal current and rise time of 100us, has been used to excite the coil. With a time step $\Delta t = 1.3096\cdot 10^{-7}$, it took around 16 min of CPU time and 37.3 MB of computer memory to calculate the transient electromagnetic field up to 2 ms in duration. The FDTD results provide data on the total field inside the conductor (superposition of primary and secondary field). The primary field can be computed with Bio-Savart's Law or the FDTD method with no conductors in the computational domain and then subtracted from the total field to obtain the secondary eddy current field. The simulation results are illustrated in Figure 1. For detailed temporal eddy current results from a range of gradient coil designs, please refer to paper (Trakic *et al*, FDTD Analysis of transient eddy currents induced by gradient coil switching in MRI, *ISMRM 2006*, submitted).

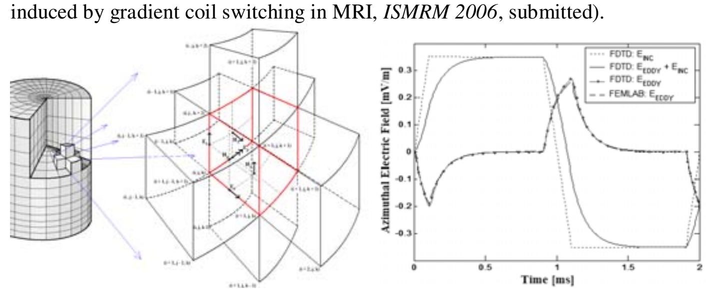

Figure 1 – Arrangement of EM-field components in cylindrical Yee cell (left); Transient validation result of azimuthal electric field inside the conductor (E_{INC} is the incident, $E_{INC+EDDY}$ is the total and E_{EDDY} is the eddy current azimuthal electric field inside the conductor, respectively)

Conclusion: A prototype '*c*-downscaled' FDTD algorithm in 3D cylindrical coordinates for the analysis of temporal low-frequency eddy current fields has been presented. A targeted application is the combined optimisation of gradient coils and magnet geometries as well as the preselection of initial pre-emphasis and B0 compensation waveforms.

Acknowledgement: Financial support for this project from the Australian Research Council is gratefully acknowledged.

References:

[1] C. Cangellaris *et al*., *IEEE Trans. Anten..Prop.*,**39** (1991), 1518-1525
[2] A. Taflove, *Computational Electrodynamics,* 1995
[3] R. Holland *et al*., *IEEE Trans. Elec. Comp.,* **36**, 1 (1994), 32-39
[4] F. Liu *et al*. *IEEE Trans. Appl. Supercon*., 14, 3 (2004), 1983-1989